Cover Page

Crystallographic interdigitation in oyster shell folia enhances material strength

Yuan Meng,[†] Susan C. Fitzer,[#] Peter Chung,[§] Chaoyi Li,[†] Vengatesen Thiyagarajan,[†,*] and Maggie Cusack[‡,*]

[†]The Swire Institute of Marine Sciences and School of Biological Sciences, The University of Hong Kong, Hong Kong Special Administrative Region.

[#]Institute of Aquaculture, Faculty of Natural Sciences, University of Stirling, Pathfoot Building, Stirling, FK9 4LA, UK

[§] School of Geographical and Earth Sciences, University of Glasgow, Glasgow, G12 8QQ, UK

[‡]Division of Biological & Environmental Sciences, Faculty of Natural Sciences, University of Stirling, Cottrell Building, Stirling, FK9 4LA, UK

ABSTRACT: Shells of oyster species belonging to the genus *Crassostrea* have similar shell micro-structural features comprising well-ordered calcite folia. However, the mechanical strengths of folia differ dramatically between closely-related species. For example, the calcareous shells of the Hong Kong oyster *Crassostrea hongkongensis*, are stronger than those of its closest relative, the Portuguese oyster, *Crassostrea angulata*. Specifically, after removal of organic content, the folia of *C. hongkongensis* are 200% tougher and able to withstand a 100% higher crushing force than that of *C. angulata*. Detailed analyses of shell structural and mechanical features support the hypothesis that crystallographic interdigitations confer elevated mechanical strength in *C. hongkongensis* oyster shells compared to *C. angulata* shells. Consequently, the folia of *C. hongkongensis* is structurally equipped to withstand higher external load compared to *C. angulata*. The observed relationships between oyster shell structure, crystallography and mechanical properties provided an insightful context in which to consider the likely fate of these two species in future climate change scenarios. Furthermore, the interdisciplinary approach developed in this study through integrating electron backscatter diffraction (EBSD) data into finite element analysis (FEA) could be applied to other biomineral systems to investigate the relationship between crystallography and mechanical behavior.

*** Corresponding Authors**

V Thiyagarajan: rajan@hku.hk

Maggie Cusack: maggie.cusack@stir.ac.uk

Crystallographic interdigitation in oyster shell folia enhances material strength

Yuan Meng,[†] Susan C. Fitzer,[#] Peter Chung,[§] Chaoyi Li,[†] Vengatesen Thiyagarajan,[†,*] and Maggie Cusack[‡,*]

[†]The Swire Institute of Marine Sciences and School of Biological Sciences, The University of Hong Kong, Hong Kong Special Administrative Region.

[#]Institute of Aquaculture, Faculty of Natural Sciences, University of Stirling, Pathfoot Building, Stirling, FK9 4LA, UK

[§] School of Geographical and Earth Sciences, University of Glasgow, Glasgow, G12 8QQ, UK

[‡]Division of Biological & Environmental Sciences, Faculty of Natural Sciences, University of Stirling, Cottrell Building, Stirling, FK9 4LA, UK

*** Corresponding Authors**
V Thiyagarajan: rajan@hku.hk
Maggie Cusack: maggie.cusack@stir.ac.uk

ABSTRACT: Shells of oyster species belonging to the genus *Crassostrea* have similar shell micro-structural features comprising well-ordered calcite folia. However, the mechanical strengths of folia differ dramatically between closely-related species. For example, the calcareous shells of the Hong Kong oyster *Crassostrea hongkongensis*, are stronger than those of its closest relative, the Portuguese oyster, *Crassostrea angulata*. Specifically, after removal of organic content, the folia of *C. hongkongensis* are 200% tougher and able to withstand a 100% higher crushing force than that of *C. angulata*. Detailed analyses of shell structural and mechanical features support the hypothesis that crystallographic interdigitations confer

elevated mechanical strength in *C. hongkongensis* oyster shells compared to *C. angulata* shells. Consequently, the folia of *C. hongkongensis* is structurally equipped to withstand higher external load compared to *C. angulata*. The observed relationships between oyster shell structure, crystallography and mechanical properties provided an insightful context in which to consider the likely fate of these two species in future climate change scenarios. Furthermore, the interdisciplinary approach developed in this study through integrating electron backscatter diffraction (EBSD) data into finite element analysis (FEA) could be applied to other biomineral systems to investigate the relationship between crystallography and mechanical behavior.

Keywords: biomineralization; oyster shell; *Crassostrea hongkongensis*; *C. angulata*; crystal orientation; electron backscatter diffraction, finite element analysis; shell mechanical strength

■ INTRODUCTION

Edible oysters belonging to the genus *Crassostrea*, herein referred to as "oysters", build mechanically strong $CaCO_3$ shells using biologically controlled biomineralization processes. These shells protect them from predators and provide substrates and shelters for others organisms.[1] Oyster shells are composite structures primarily composed of calcium carbonate ($CaCO_3$) crystal units with a minor fraction of organic material.[2, 3] The hierarchical structures and orientated crystalline structures result in material properties that enable biomineralized structures such as oyster shells to be light and strong and perform a protective function for the organism.[4, 5] These complex structures have been refined through evolution and speciation.[6] Consequently, each oyster species may have developed a unique way of assembling their crystal units to achieve superior mechanical strengths for minimal energy expenditure and maximal weight gain.[7, 8] Thus, structural features of each oyster species may hold rich information to inspire the development of novel biomaterials for construction and biomedical applications.[9] Despite their potential applications in applied and basic science, only a small number of studies have examined the genetically controlled relationships between shell structural and mechanical features in oyster species that tend to build shells with contrasting mechanical strength and in commercially important edible oyster species inhabiting along the coastal areas of China.[10, 11]

Generally, oyster shells are comprised mainly of calcitic folia with some calcitic chalk.[3, 12-15] Folia can be considered as the calcite analogue of nacre with overall uniform crystallography across the Bivalvia (Figure 1).[5, 12-14] It has been well established that the mineral composition of oyster shell contributes to its mechanical strength.[3, 16] However, the microstructural properties of shells: the size, shape, and orientation of crystallographic mineral units, can also significantly contribute to the mechanical strength.[10] A strong correlation between crystal unit morphology and orientation and mechanical strength is expected because resistance to fracture generation increases with decreasing crystal unit size

and increasing orientation complexity.[17, 18] Thus, increased microstructural complexity of crystal units, especially in the folia layer of oyster shell, can result in enhanced mechanical strength. However, only a few studies have attempted to understand the influence of microstructure, such as crystal unit size, shape and orientation, on the mechanical properties of oyster shells.[10] For example, irregularly and loosely arranged crystal units in the chalky layer resulted in a brittle structure with reduced hardness 30 times lower than the folia layer.[19, 20] Although these studies provide information about shell microstructure and mechanical properties, we still do not know how crystal orientation influences the mechanical properties of the folia of different edible oyster species. In addition, we do not know how the closely related oyster species differ in their shell microstructural design and thus in their mechanical properties. Studying edible oysters living in Chinese coastal waters provides an opportunity to fill this knowledge gap.

The Hong Kong (HK) oyster, *Crassostrea hongkongensis* and the Portuguese oyster, *C. angulata*, are widely distributed and commercially cultivated along the coastal and river mouths of Southern China.[21] While *C. hongkongensis* is considered to be endemic to the region, the Portuguese oyster has been successfully introduced to Europe via Portugal.[22] The Portuguese oyster is morphologically indistinguishable from the Pacific oyster, *C. gigas*.[23] These two commercially important species have high genome similarity and inhabit similar habitats i.e. estuarine river mouths of South China coastal areas, yet appear to have strikingly different structural and mechanical features (Figure S1). What underpins these differences in shell mechanical characteristics between these two closely related oyster species? Focusing on folia, the most abundant shell component, we used micro-computed tomography (Micro-CT) to quantify the proportion of folia, micro-force loading to quantify the mechanical resistance corresponding to the crushing force, electron backscatter diffraction (EBSD) to determine crystallographic orientation and finite element analysis (FEA) to determine the fracture stress of folia in these two species. This innovative combination of materials science techniques

enables us to directly interpret the influence of crystallography on the material properties of biogenic calcite.

■ EXPERIMENTAL SECTION

Shell sample collection. Adult shells of the HK oyster (*C. hongkongensis*) and the Portuguese oyster (*C. angulata*) were collected from the naturally recruited populations in coastal areas of Southern China (Guangdong province, South China). The shell height, length and width of *C. hongkongensis* were 52±6, 33±6, and 20±4 mm, respectively. The size measurements of the collected Portuguese oyster shells were similar to *C. hongkongensis*, i.e. the shell height, length and width were 51±7, 38±4 and 27±5 mm, respectively. The age of the oyster shell specimens were 12 to 15 months.

Shell ultrastructure. Fractured shell sections were glued to scanning electron microscopy (SEM) stubs and gold-coated. Secondary electron images were collected with a beam voltage of 5kV at a working distance of 9 mm in high vacuum mode on the Sigma Variable Pressure Analytical SEM.

Shell structural composition. Shell structural compositions of both valves were compared in terms of the percentage of folia in the oyster shells by using high-resolution Micro-CT (Micro-CT, SkyScan 1076, Skyscan, Belgium) with a spatial resolution of 9 μm. Shells were placed in Falcon tubes and held in the chamber of the Micro-CT scanner securely. The three-dimensional digital information was converted to shell surface topography, mineral density and corresponding volume obtained as ~2000 two-dimensional layers. The shell density and volume were measured by comparison with standard phantoms that are used for bone density measurement[24] analytical software CT-Analyser v 1.14.4.1 (SkyScan, Kontich, Belgium). To calibrate the identification of foliated and chalky layers, the shells were sectioned after scanning and folia and chalk identified by eyes. The mineral density range of folia, ~ >1.5 g/cm^3, and the corresponding partial volume were then used to calculate the

percentage of folia. Shells from four individuals per species were analyzed by Micro-CT scanning.

Mechanical characteristics of shell "folia" layer. Crushing test was used to examine the mechanical characteristics of folia, including the crushing force which represented the mechanical strength or resistance and toughness which represented the energy required for material failure or fracture.[25-27] A standardized shell specimens were used here to ensure the comparability. An oyster has two calcareous shell valves, the cemented (on substratum) cupped or left valve and the lid or flat right valve. The deep cup-shaped left valve is more prone to cracking since it morphogenetically concentrates more stress at the hinge region under external load.[11, 28] Therefore, the folia from the hinge region of the left valve were analyzed for mechanical strength (or resistance) and toughness corresponding to the crushing test. First, the hinge section of the oyster shell (left valve) was cut out using a hand saw. Then, a folia plate of 1 mm in height was sectioned by polishing the inner and outer surfaces of the hinge section using grit paper (P240). Finally, a 1 mm^3 cubic specimen was cut out from this plate using an automatic diamond saw blade. One specimen was obtained from one individual. In total, fifteen specimens or replicate samples were used per species of oyster, among which five specimens were immersed in 5% sodium hypochlorite for two hours to remove organic content from cubic folia specimens. These five specimens were examined before and after incubating in sodium hypochlorite under SEM to confirm the removal of organic content (Figure S2)[20].

The crushing test was conducted with the micro-force testing system (Tytron 250, MTS System Co., USA) equipped with a Test Star II controller. Two circular metal plates (diameter of 1.5 cm) were parallel clamped to the actuator and force transducer respectively. The specimen was mounted on the metal plate clamped to the force transducer to ensure that the thickness direction of the shell coincides with the crushing direction. The displacement control load with speed of 0.05 mm/sec was applied.

Folia composition in terms of organic and magnesium content. As the small occluded fraction of organic matrix and magnesium content is expected to play an important role in determining shell mechanical properties, these two characteristics of folia were evaluated and compared between the two oyster species. Folia organic matter content was determined by the weight loss percentage of the folia after ignition.[29] The folia were sectioned and prepared as previously described for the crushing force test. The extractable folia were powdered manually for 15 min with a glass pestle and mortar. The folia powder collected in pre-weighed crucibles were oven dried at 60°C for 24 hours and weighed to determine the dry weight (DW). Samples were placed in a furnace at 500°C and weighed to determine the ash weight (AW) in terms of the inorganic content. Ash-free dry weight (AFDW) in terms of organic content was obtained as the weight loss from DW to AW and the weight loss percentage was calculated as the proportion of AFDW to DW.[29] One specimen was obtained from one individual. In total, ten specimens or replicate samples were used per species of oyster.

The folia cubes after removal of organic content in the same way which described in the crushing test section were used for the evaluation of magnesium content using a scanning electron microscope (SEM; Hitachi S-3400N VP SEM, Hitachi, Japan) with integrated energy dispersive X-ray spectroscopy (EDS) system for elemental analysis. Specimen analysis was carried out on carbon-coated folia cubes after removal of organic content. All was analyses were carried out using a magnification of 5000 with acquisition time of 30 seconds. Six to seven specimens of each species with three sites of interest per specimen were used for the EDS analysis. At each site of interest, five spectra were accumulated, and the mean values were obtained for each site. The value for each specimen was calculated by the average of the values of three site.

Electron backscatter diffraction analysis. The crystal orientation of the folia of oyster shells was examined using electron backscatter diffraction (EBSD), a microstructural-

crystallographic analysis technique. Left valves of two species of oyster shells were coated using epoxy resin (EpoxyCure, Buehler) and sliced transversely at low speed using a diamond trim saw blade to section the entire length of the shell. The sliced longitudinal sections of the oyster shells were sectioned into 4-5 parts depending on the length of the shell. Shell sections were then embedded separately into epoxy resin blocks and polished by hand for 2–4 min using grit papers (P320, P800, P1200, P2500, and P4000), followed by further polishing for 4 min on cloths using 1 μm and 0.3 μm alpha alumina, and for 2 min using colloidal silica to ensure a smooth shell surface. Polished shell sections were analyzed using EBSD to determine crystallographic orientation. A beam voltage of 20 kV was applied under low vacuum mode (~50 Pa) on an FEI Quanta 200F with the stage tilted to 70° to examine backscatter Kikuchi patterns.[30] Diffraction intensity, phase and crystallographic orientation maps were produced through OIM Analysis 6.2 software. Data points with a confidence index of less than 0.1 were removed. EBSD results are presented as crystallographic orientation maps and pole figures with each color in the maps and pole figures representing a particular crystallographic orientation. Pole figures were examined for spread of crystallographic orientation using 5° angle gridlines.[31] Two specimens or replicate samples were examined per species of oyster.

Calculation of stiffness tensors of shell folia. The average elastic stiffness tensors of polyphase aggregates of folia were calculated for each species by MTEX, a freely available Matlab© toolbox for quantitative texture analysis[32]. By inputing the crystallographic texture of calcite-unit acquired from EBSD in the same coordinate system and the anisotropic elastic tensor of single-crystal calcite[33], the collected elastic features of calcite-unit, average elastic stiffness tensors, were calculated. Table 1 shows the values of two species in Voigt notation.

Finite element modelling analysis of shell folia. In order to model the mechanical responses of shell folia of the two oyster species, finite element analysis (FEA) was conducted using the software ABAQUS/standard (Dassault Systems, France). In this model, a 1 mm^3 3D "folia" cube with a fixed bottom surface was compressed from the top by a rigid plane. The

elastic stiffness tensors calculated in the last section were assigned to the "folia" cube with setting the y-axis parallel to the compressing direction for coinciding with the scenario of the crushing test. Quadratic brick element (C3D20 in ABAQUS) was assigned for the 3D cube in the simulations.

Statistical analysis. One-way ANOVA was used to examine the proportion of folia and chalk between two oyster species (n = 4), the crushing force of the folia cubic specimen without organic content (n = 5), the toughness of the folia cubic specimen after the removal of organic content (n = 10) and the magnesium content in folia (n = 6 and 7). Before this statistical analysis, data were checked for normality and homogeneity of variance assumptions. If the data did not pass those ANOVA assumptions, a non-parametric ANOVA analysis (Mann-Whitney U test) was used to examine the crushing force of the folia cubic specimen before the removal of organic content (n = 10), the toughness of the folia cubic specimen after the removal of organic content (n = 5) and the weight loss percentage of folia under ignition (n = 10).

■ RESULTS

Proportion of folia in oyster shells. The Micro-CT analyses reveal that the foliated layer of *C. hongkongensis* is more compact than that of *C. angulata* and the foliated layers of *C. angulata* are more frequently interrupted by enclosed pores of chalky lenses (Figures 2a-d). Shells of *C. hongkongensis* have more folia (~70 %), and correspondingly less chalk, when compared to the shells of *C. angulata* (~60 %) (Figure 2e). The shells of *C. hongkongensis* had a significantly higher proportion of folia when compared to the shells of *C. angulata* ($F_{(1, 6)} = 44.97$, $p < 0.05$).

Folia mechanical characteristic. The mechanical characteristics of the folia before and after removal of organic content of shells of two oyster species quantified by the crushing test depicted in the experimental section. Based on the displacement (mm) - force (N) curve

obtained by each test (Figure 3a and b), the crushing force was defined by the corresponding force of the data point before a sharp change of force occurred due to the sample failure which represents the resistance or strength of the folia cube (Figures 3b).[34] Before demonstrating this result further, it was necessary to define toughness, which is commonly used to characterize the mechanical properties in the field of fracture mechanics.[25-27] In our cases, the toughness represents the input energy inducing the totally crush of the folia cube. In other words, a higher toughness means more energy is required for the fracture or failure, indicating that the material is harder to fracture. As shown in Figure 3b, the toughness was depicted as the area enclosed by the displacement (mm) - force (N) curve and the horizontal axis to the failure point, which is expressed as:

$$\text{Toughness} = \int_0^{\varepsilon_f} \sigma d\varepsilon = \frac{\int_0^{S_f} F dS}{V}$$

where ε is the strain, ε_f is the strain upon failure, σ is the stress, V is the volume of the folia cube which is approximately equal to $1\,mm^3$, F is the force (N) applied on the top surface of folia cube, S is the displacement (mm) of the top surface of folia cube, S_f is the displacement (mm) upon failure.

Therefore, firstly, whether or not organic material has been removed from folia cubes, the folia of *C. hongkongensis* required a significantly higher crushing force than those of *C. angulata* (before the removal of organic content: Mann-Whitney U test, $p < 0.05$; after the removal of organic content: $F_{(1, 8)} = 7.87$, $p < 0.05$) (Figure 3c). This indicates that the mechanical strength or resistance of the folia of *C. hongkongensis* was higher than those of *C. angulata*. Secondly, although there is no difference in the toughness of the folia upon the removal of organic content between the two oyster species ($F_{(1, 18)} = 0.12$, $p > 0.05$), the folia of *C. hongkongensis* after the removal of organic content were significantly tougher than those of *C. angulata* (Mann-Whitney U test, $p < 0.05$) (Figure 3d).

Folia composition in terms of organic matter and magnesium content. The folia of *C. hongkongensis* had a significantly lower organic content than folia of *C. angulata* (Mann-Whitney U test, $p < 0.05$) (Figure 4a). Meanwhile, there was no significant difference of magnesium content in folia of *C. hongkongensis* and *C. angulata* ($F_{(1,11)} = 1.552$ $p > 0.05$) (Figure 4b).

Crystallography of the folia. The orientation of the crystal units in the foliated layer at the hinge sections of *C. hongkongensis* and *C. angulata* shells were quantitatively compared using EBSD analysis (Figure 5). Crystallographic orientation maps indicate that *C. hongkongensis* has less crystallographic constraint on folia compared to *C. angulata* (Figures 5a and b). The calcite crystal units of *C. hongkongensis* were frequently interdigitated when compared to *C. angulata* (Figure 5b), the latter showing more uniform crystal arrangement patterns. The pole figures also highlighted the lower crystallographic constraint in *C. hongkongensis* when compared to *C. angulata*. The pole figures indicate a higher scattering of crystallographic orientation as per the orientation maps in *C. hongkongensis*, compared to *C. angulata* shells which have more uniform clustering of crystal orientation (Figure 5c).

Finite element analysis of folia. The finite element analysis (FEA) results are shown in Figure 6. When 46.8 N compressive force (average crushing force for folia cubes of *C. angulata* after removal of organic content) was applied on the top rigid plate, the largest maximum principal (MP) stress and MP strain occurred at the corner of both folia cubes regardless of the oyster species (Figures 6a and b). However, the distribution of MP stress and MP strain of the folia in *C. hongkongensis* shells is more uniform than that of *C. angulata*. The corresponding maximum values of MP stress are 0.20 GPa and 0.24 GPa, as well as that of MP strain are 0.0016 and 0.0021 for *C. hongkongensis* and *C. angulata*, respectively (Figures 6a and b).

The developing maximum values of MP stress and MP strain of the folia cubes of the two species under compressive loading are summarized in Figure 6c. The folia of *C.*

hongkongensis always concentrate less stress and strain than those of *C. angulata* with the same compressive loading. In order words, with the same value of MP stress and MP strain, the folia of *C. hongkongensis* can sustain larger external compressive forces than *C. angulata* (Figure 6c).

In order to investigate the toughness, the displacement (mm) - applied load (N) curve was displayed in Figure 6d. In accordance with the definition of toughness introduced in previous results of crushing test, the simulated toughness in FEA was depicted as the area enclosed by the displacement (mm) – applied load (N) curve (Figure 6d).

Based on the Figure 6c and 6d,

$$\text{Toughness} = \frac{\sigma_{\text{MP}}^2}{2 \times k_{S-F} \times k_{F-\sigma_{\text{MP}}}{}^2}$$

$$\text{Toughness} = \frac{\varepsilon_{\text{MP}}^2}{2 \times k_{S-F} \times k_{F-\varepsilon_{\text{MP}}}{}^2}$$

where σ_{MP} is the MP stress, ε_{MP} is the MP strain, $k_{F\text{-}\varepsilon}$, $k_{F\text{-}\sigma}$, $k_{S\text{-}F}$ are the slopes of the applied load (N) - MP stress (GPa) curve, the applied load (N) - MP strain curve and the displacement (mm) - applied load (N) curve, respectively (Figures 6c and d).

The MP stress (GPa) -toughness (mJ) curves and the MP stress - toughness (mJ) curves were summarized in Figure 6e and 6f. It is clear that, whether failure criteria of MP stress or MP strain is used,[25-27] the folia of *C. hongkongensis* required higher energy for fracture or failure than those of *C. angulata*, which indicated that the folia of *C. hongkongensis* had higher toughness (i.e. required higher energy) than that of *C. angulata* (Figures 6e and f). Because the only difference between two species in FEA is the elastic stiffness tensor (calculated in the experimental section) according to different crystallographic textures of calcite, this reveals that the crystallographic texture of calcite in the foliated layer has a significant effect on the mechanical strength and toughness of oyster shell.

■ DISCUSSION

This study demonstrated the relationship between microstructural and mechanical properties of shells of the two oyster species that have contrasting mechanical strength but similar morphology, size and shape. The foliated layers of *C. hongkongensis* are biologically assembled to be stronger (withstand a greater crushing force) than *C. angulata.* This finding persists whether or not organic material is removed. Importantly, this greater strength is achieved with significantly less organic matrix and similar magnesium content in folia of *C. hongkongensis* than *C. angulata*. After removal of the organic content, the foliated layers of *C. hongkongensis* are 200% tougher than those of *C. angulata*, which highlights the fact that the crystallographic texture may contribute to this enhanced mechanical property. Subsequent analysis of crystal orientation using EBSD provided a possible explanation for such a striking difference in mechanical strength between the two species. For example, crystal units of the *C. hongkongensis* folia layer varied highly in their orientation, ultimately producing an interdigitation of the crystals. In contrast, the crystal units in the folia of *C. angulata* have more uniform orientation. This relationship between crystal unit orientation and mechanical behavior in oyster species was further confirmed by finite element analysis (FEA). Thus, our study indicates that in contrast to *C. angulata*, the shells of *C. hongkongensis* with a microstructure that is formed by interlocking complex crystal units, are tougher and able to withstand the higher crushing force or predatory attack than *C. angulata* shells of similar size. Similarly, the propensity for microstructural microcracking is confirmed to be reduced in calcitic marble by increasing the crystal preferred orientations.[35]

Although shell mechanical strength is primarily determined by microstructural features and orientation of crystal units, the occluded small fraction of organic matrix also plays an important role in ultimately determining the shell mechanical properties, such as hardness, fracture toughness, and elasticity.[36] Therefore, this study not only quantified the total fraction of organic matrix components of the folia from the two oyster species but also evaluated and compared the strength (crushing force) and toughness of folia before and after removal of

organic content. In contrast to our expectation, the mechanically stronger shells of *C. hongkongensis* had less organic matrix than the weaker shells of the *C. angulata*. The organic matrix between intercrystallite and nanograins in folia of oyster shells is organized in a foam-like structure.[20] Such foam-like structural units within the folia layer are expected to enhance the shell toughness and strength through reducing the area of the cleavage plane in crystals.[37] The *C. angulata* shells with a significantly higher amount of organic components are mechanically weaker than the shells of *C. hongkongensis* which have a lower amount of organic components. With such a lower resistance to external load, the higher organic content may be more important for *C. angulata*, to rescue some toughness for *C. angulata* shell. This comparative analysis suggests that the crystallographic interdigitation has a greater effect on determining shell mechanical strength when compared to total organic content. Similarly, the significance of crystallographic orientation within shell microstructures to determine material mechanical properties has been highlighted in both non-biogenic[38] and biogenic shell materials.[30]

The existing relationship between crystal unit orientations or assemblages and mechanical strength in oyster shells was further explored through FEA analysis. According to our FEA modelling analysis, interdigitation of crystal units in the folia of *C. hongkongensis* enables the shells to always concentrate less stress and strain under the same external loading and requires higher energy for failure when compared to the uniformly assembled crystals in the shells of *C. angulata*. The results of this study have implications for biomaterial research. For example, by directly determining the influence of crystallography on the material properties of biogenic calcite, the unique material properties and crystallographic interdigitations that are found in folia of *C. hongkongensis* could inform the design of biomaterials with predetermined material properties. This could be used to develop an oyster-derived scaffold with superior biomechanical properties for bone development and

regeneration and inspire the design of material with enhanced mechanical properties by optimizing the crystallography.

The ability to scale up the material properties is important if we are to be able to forecast the modulating effect of environmental changes such as climate change (ocean acidification and global warming) on oyster shell material properties. From an ecological perspective, *C. angulata* produces a mechanically weaker shell under near future climate change conditions such as elevated CO_2 and decreased pH and would be expected to be more susceptible to predatory attack.[39]

The mechanical modelling approach developed in this study using EBSD data integrated with FEA models could be easily applied to other biomineral systems to investigate the relationship between structural and mechanical properties in biological constructs.

■ CONCLUSION

In nature, many organisms have evolved to control biomineralization for mechanical support and protection. As the main shell component, folia of *C. hongkongensis* exhibit superior strength and toughness compared with *C. angulata*. This advanced mechanical strength and toughness was attributed to the crystallographic interdigitations in the folia of *C. hongkongensis*. Crystallographic interdigitations found in this study may provide an inspiration for the synthesis of biomaterials with enhanced fracture toughness.

■ AUTHOR INFORMATION

Corresponding Author

*Author to whom correspondence should be addressed: E-Mail: maggie.cusack@stir.ac.uk, Tel.: +44 (0)1786467855; web: www.stir.ac.uk/people/34665

Notes

The authors declare no competing financial interest.

■ **ACKNOWLEDGEMENTS**

Access to the micro-force loading test and ABAQUS was provided through Dr. Yao Haimin (The Hong Kong Polytechnic University, Hong Kong), with assistance through Mr. Fu Jimin and Mr. Guo Zhenbin. MC thanks Scottish Universities Life Science Alliance (SULSA) and the Scottish Funding Council for funding this Hong Kong: Scotland Collaborative Research Partnership Award (2014_HK-Scot-0038). SF acknowledges the support of the University of Glasgow Principal's Early Career Mobility Scheme. This study was supported by RGC grants (705511P and 15219314), SKLMP Seed Collaborative Research Fund (2017) (SKLMP/SCRF/0019) and SFC / RGC Joint Research Scheme (X_HKU704/14) to VT.

■ REFERENCES

(1) Marenghi, F. P.; Ozbay, G. Floating oyster, *Crassostrea virginica* Gmelin 1791, aquaculture as habitat for fishes and macroinvertebrates in Delaware Inland Bays: the comparative value of oyster clusters and loose shell. *J. Shellfish Res.* **2010,** *29* (4), 889-904.

(2) Marin, F.; Luquet, G.; Marie, B.; Medakovic, D. Molluscan shell proteins: primary structure, origin, and evolution. *Curr. Top. Dev. Biol.* **2008,** *80*, 209-276

(3) Dauphin, Y.; Ball, A. D.; Castillo-Michel, H.; Chevallard, C.; Cuif, J.-P.; Farre, B.; Pouvreau, S.; Salomé, M. *In situ* distribution and characterization of the organic content of the oyster shell *Crassostrea gigas* (Mollusca, Bivalvia). *Micron* **2013,** *44* (Supplement C), 373-383.

(4) Lin, A. Y. M.; Meyers, M. A.; Vecchio, K. S. Mechanical properties and structure of *Strombus giga*, *Tridacna gigas*, and *Haliotis refuscens* sea snails: A comparative study. *Mater. Sci. Eng., C* **2006,** *26* (8), 1380-1389.

(5) MacDonald, J.; Freer, A.; Cusack, M. Alignment of crystallographic *c*-axis throughout the four distinct microstructural layers of the oyster *Crassostrea gigas*. *Cryst. Growth Des.* **2010,** *10* (3), 1243-1246.

(6) Kocot, K. M.; Aguilera, F.; McDougall, C.; Jackson, D. J.; Degnan, B. M. Sea shell diversity and rapidly evolving secretomes: insights into the evolution of biomineralization. *Front. Zool.* **2016,** *13*, 23.

(7) Lord, J.; Whitlatch, R. Latitudinal patterns of shell thickness and metabolism in the eastern oyster *Crassostrea virginica* along the east coast of North America. *Mar. Biol.* **2014,** *161* (7), 1487-1497.

(8) Chen, P. Y.; Lin, A. Y. M.; Lin, Y. S.; Seki, Y.; Stokes, A. G.; Peyras, J.; Olevsky, E. A.; Meyers, M. A.; McKittrick, J. Structure and mechanical properties of selected biological materials. *J. Mech. Behav. Biomed. Mater.* **2008,** *1* (3), 208-226.

(9) Yang, Y.; Yao, Q.; Pu, X.; Hou, Z.; Zhang, Q. Biphasic calcium phosphate macroporous scaffolds derived from oyster shells for bone tissue engineering. *Chem. Eng. J.* **2011,** *173* (3), 837-845.

(10) Lee, S. W.; Kim, G. H.; Choi, C. S. Characteristic crystal orientation of folia in oyster shell, *Crassostrea gigas*. *Mater. Sci. Eng. C Biomimetic Supramol. Syst.* **2008,** *28* (2), 258-263.

(11) Lombardi, S. A.; Chon, G. D.; Lee, J. J. W.; Lane, H. A.; Paynter, K. T. Shell hardness and compressive strength of the eastern oyster, *Crassostrea virginica*, and the asian oyster, *Crassostrea ariakensis*. *Biol. Bull.* **2013,** *225* (3), 175-183.

(12) Boggild, O. B. The shell structure of the mollusks. *D. Kgl. Danske Vidensk. Selsk. Skr. Naturevidensk. Og Mathem. Afd.* **1930,** *9*, 231-236.

(13) Taylor, J. D. The shell structure and mineralogy of the Bivalvia. Introduction. Nuculacea-Trigonacea. *Bull. Br. Mus. Nat. Hist. (Zool.)* **1969,** *3*, 1-125.

(14) Checa, A. G.; Esteban-Delgado, F. J.; Rodriguez-Navarro, A. B. Crystallographic structure of the foliated calcite of bivalves. *J. Struct. Biol.* **2007,** *157* (2), 393-402.

(15) Mouchi, V.; Lartaud, F.; Guichard, N.; Immel, F.; de Rafélis, M.; Broussard, C.; Crowley, Q. G.; Marin, F. Chalky versus foliated: a discriminant immunogold labelling of shell microstructures in the edible oyster *Crassostrea gigas*. *Mar. Biol.* **2016,** *163* (12), 256.

(16) Choi, C. S.; Kim, Y. W. A study of the correlation between organic matrices and nanocomposite materials in oyster shell formation. *Biomaterials* **2000,** *21* (3), 213-222.

(17) Feng, Q. L.; Cui, F. Z.; Pu, G.; Wang, R. Z.; Li, H. D. Crystal orientation, toughening mechanisms and a mimic of nacre. *Mater. Sci. Eng. C Biomimetic Supramol. Syst.* **2000,** *11* (1), 19-25.

(18) Li, X. D.; Chang, W. C.; Chao, Y. J.; Wang, R. Z.; Chang, M. Nanoscale structural and mechanical characterization of a natural nanocomposite material: The shell of red abalone. *Nano Lett.* **2004,** *4* (4), 613-617.

(19) Lee, S. W.; Jang, Y. N.; Ryu, K. W.; Chae, S. C.; Lee, Y. H.; Jeon, C. W. Mechanical characteristics and morphological effect of complex crossed structure in biomaterials: fracture mechanics and microstructure of chalky layer in oyster shell. *Micron* **2011,** *42* (1), 60-70.

(20) Lee, S. W.; Kim, Y. M.; Kim, R. H.; Choi, C. S. Nano-structured biogenic calcite: A thermal and chemical approach to folia in oyster shell. *Micron* **2008,** *39* (4), 380-6.

(21) Lam, K.; Morton, B. Mitochondrial DNA and morphological identification of a new species of *Crassostrea* (Bivalvia : Ostreidae) cultured for centuries in the Pearl River Delta, Hong Kong, China. *Aquaculture* **2003,** *228* (1-4), 1-13.

(22) Arakawa, K. Y. Commercially important species of oysters in the world. *Mar. Freshwat. Behav. Physiol.* **1990,** *17* (1), 1-13.

(23) Wang, H.; Qian, L.; Liu, X.; Zhang, G.; Guo, X. Classification of a Common Cupped Oyster from Southern China. *J. Shellfish Res.* **2010,** *29* (4), 857-866.

(24) Celenk, C.; Celenk, P. Bone density measurement using computed tomography. In *Computed Tomography - Clinical Applications*, Saba, L., Ed. InTech: Rijeka, Croatia, 2012; pp 123-136.

(25) Anderson, T. L. *Fracture mechanics: fundamentals and applications*. second ed.; CRC press: Boca Raton, FL, 1995.
(26) Paterson, M. S.; Wong, T.-f. *Experimental rock deformation-the brittle field*. second ed.; Springer Science & Business Media: Berlin Heidelberg, 2005.
(27) Wiebols, G. A.; Cook, N. G. W. An energy criterion for the strength of rock in polyaxial compression. *Int. J. Rock Mech. Min. Sci. Geomech. Abstr.* **1968,** *5* (6), 529-549.
(28) Tiwary, C. S.; Kishore, S.; Sarkar, S.; Mahapatra, D. R.; Ajayan, P. M.; Chattopadhyay, K. Morphogenesis and mechanostabilization of complex natural and 3D printed shapes. *Sci. Adv.* **2015,** *1* (4).
(29) Pansch, C.; Nasrolahi, A.; Appelhans, Y. S.; Wahl, M. Tolerance of juvenile barnacles (*Amphibalanus improvisus*) to warming and elevated pCO_2. *Mar. Biol.* **2013,** *160* (8), 2023-2035.
(30) Perez-Huerta, A.; Cusak, M.; Zhu, W. Assessment of crystallographic influence on material properties of calcite brachiopods. *Mineral. Mag.* **2008,** *72* (2), 563-568.
(31) Fitzer, S. C.; Phoenix, V. R.; Cusack, M.; Kamenos, N. A. Ocean acidification impacts mussel control on biomineralisation. *Sci. Rep.* **2014,** *4*, 6218.
(32) Mainprice, D.; Hielscher, R.; Schaeben, H. Calculating anisotropic physical properties from texture data using the MTEX open-source package. *Geol. Soc. Lond. Spec. Publ.* **2011,** *360* (1), 175-192.
(33) Chen, C. C.; Lin, C. C.; Liu, L. G.; Sinogeikin, S. V.; Bass, J. D. Elasticity of single-crystal calcite and rhodochrosite by Brillouin spectroscopy. *Am. Mineral.* **2001,** *86* (11-12), 1525-1529.
(34) Majeed, S. A. Effect of specimen size on compressive, modulus of rupture and splitting strength of cement mortar. *J. Appl. Sci.* **2011,** *11* (3), 584-588.
(35) Shushakova, V.; Fuller, E. R.; Siegesmund, S. Influence of shape fabric and crystal texture on marble degradation phenomena: simulations. *Environ. Earth. Sci.* **2011,** *63* (7-8), 1587-1601.
(36) Kamat, S.; Su, X.; Ballarini, R.; Heuer, A. H. Structural basis for the fracture toughness of the shell of the conch *Strombus gigas*. *Nature* **2000,** *405* (6790), 1036-1040.
(37) Okumura, T.; Suzuki, M.; Nagasawa, H.; Kogure, T. Microstructural variation of biogenic calcite with intracrystalline organic macromolecules. *Cryst. Growth Des.* **2012,** *12* (1), 224-230.
(38) Zambaldi, C.; Zehnder, C.; Raabe, D. Orientation dependent deformation by slip and twinning in magnesium during single crystal indentation. *Acta Mater.* **2015,** *91*, 267-288.

(39) Li, C.; Chan, V. B. S.; He, C.; Meng, Y.; Yao, H.; Shih, K.; Thiyagarajan, V. Weakening mechanisms of the serpulid tube in a high-CO_2 world. *Environ. Sci. Technol.* **2014,** *48* (24), 14158-67.

(40) Perez-Huerta, A.; Cusack, M. Optimizing electron backscatter diffraction of carbonate biominerals-resin type and carbon coating. *Microsc. Microanal.* **2009,** *15* (3), 197-203.

Tables and Figures

Table 1. The calculated average stiffness elastic tensor of the folia in *C. hongkongensis* and *C. angulata*, which was used in the finite element analysis model. All the tensors are in Voigt notation for the calculated tensor of a single crystal of calcite in folia.

Components in Voigt notation					
C_{11}	C_{12}	C_{13}	C_{14}	C_{15}	C_{16}
	C_{22}	C_{23}	C_{24}	C_{25}	C_{26}
		C_{33}	C_{34}	C_{35}	C_{36}
	Sym.		C_{44}	C_{45}	C_{46}
				C_{55}	C_{56}
					C_{66}
Single-crystal (GPa)					
149.4	57.9	53.5	-20.2	0	0
57.9	149.4	53.5	20.2	0	0
53.5	53.5	85.2	0	0	0
-20.2	20.2	0	34.1	0	0
0	0	0	0	34.1	-20.2
0	0	0	0	-20.2	45.75
***C. hongkongensis* (GPa)**					
131.4	53.7	53.36	0.58	4.96	-2.85
53.7	135.5	57.89	2.37	1.65	1.57
53.36	57.89	116.99	2.51	1.2	-0.14
0.58	2.37	2.51	40.85	-0.3	2.48
4.96	1.65	1.2	-0.3	35.41	1.15
-2.85	1.57	-0.14	2.48	1.15	37.75
***C. angulata* (GPa)**					
139.51	55.54	57.73	-1.08	-2.43	-5.69
55.54	110.31	53.87	-8.9	-2.95	-4.51
57.73	53.87	129.72	-11.98	-1.71	-0.97
-1.08	-8.9	-11.98	35.32	-2.15	-3.69
-2.43	-2.95	-1.71	-2.15	42.67	-3.4
-5.69	-4.51	-0.97	-3.69	-3.4	38.19

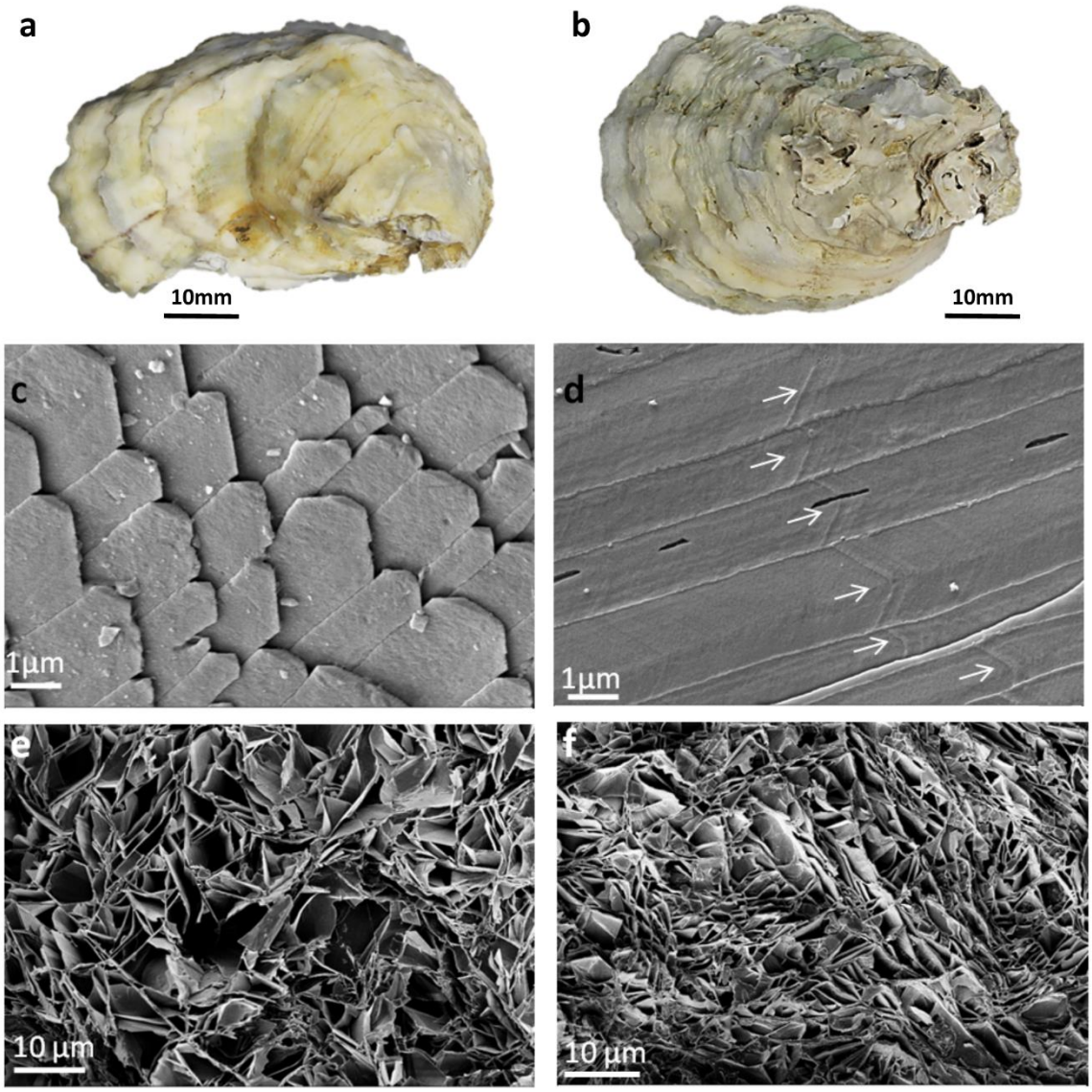

Figure 1. Shell and ultrastructure of *Crassostrea hongkongensis* and *Crassostrea angulata*. External view of shells of (a) *C. hongkongensis* and (b) *C. angulata*. Secondary electron image of shell fracture sections indicating folia and chalk respectively of (c, e) *C. hongkongensis* and (d, f) *C. angulata*. Chevron ends of folia are evident in C and the white arrows in D indicate where the chevron ends have continued to grow.

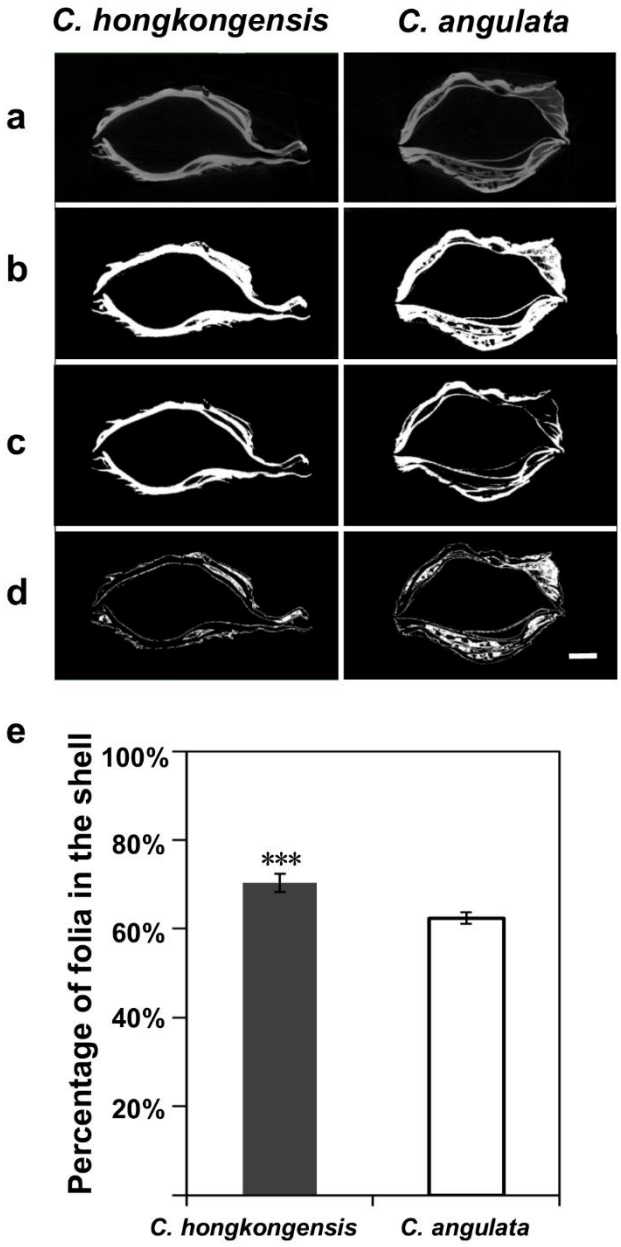

Figure 2. Micro-CT scanning analysis for percentage folia in oyster shells. (a-d) Images represent selected density ranges to determine the percentage of folia in *C. hongkongensis* and *C. angulata* shells for one section of shells as an example with the scale bar of 1 cm. The brighter white color indicates a higher density. (a) raw image of the Micro-CT scan, (b) full density range for all minerals, (c) are >1.5 g/cm^3 density range for folia, and (d) are <1.5 g/cm^3 density range for chalk. (e) Percentage of folia in the oyster shells of *C. hongkongensis* (dark grey bar) and *C. angulata* (white bar) for the entire shells, analyzed using density

fractions as shown in the examples in A-D. (Mean ± SD, n = 4).

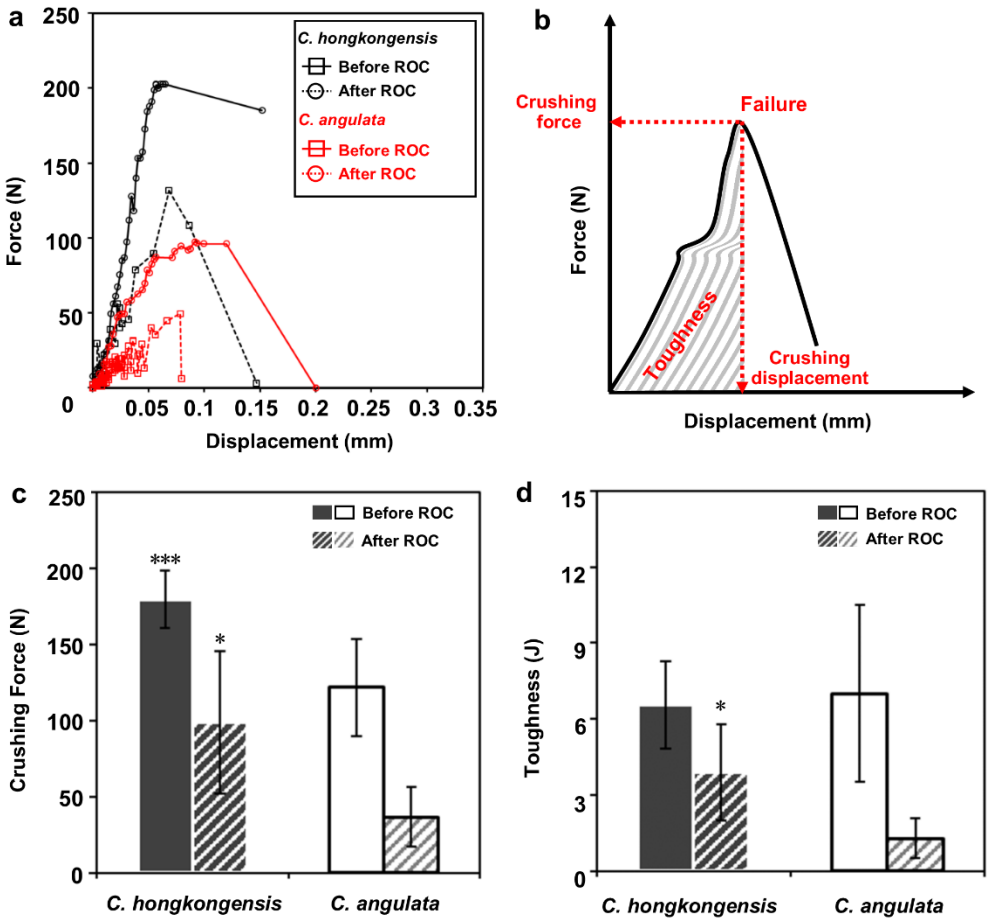

Figure 3. Mechanical characteristics including crushing force and toughness of folia in *C. hongkongensis* and *C. angulata* shells before and after the removal of organic content (ROC). (a) Representative force - displacement curve acquired from the crushing test of the folia cubes before and after ROC of the two species. (b) Schematic depicts the quantity including crushing force and toughness based on the force - displacement curve (c) Folia mechanical resistance before and after ROC according to the crushing force. (d) Toughness of the folia cubes before and after ROC of the two species. Error bars represent the mean ± SD of 10 replicates (before ROC) and 5 replicates (after ROC).

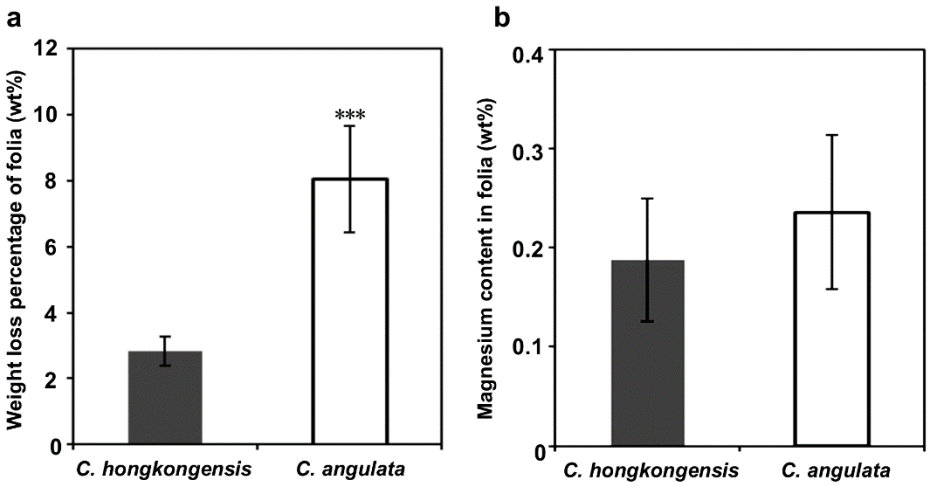

Figure 4. Folia composition of *C. hongkongensis* and *C. angulata* in terms of (a) weight loss on ignition indicating organic content and (b) magnesium content in folia acquired by elemental analysis using energy dispersive X-ray spectroscopy (EDS). Error bars represent the mean ± SD of 10 replicates in (a) and 6 or 7 replicates in (b).

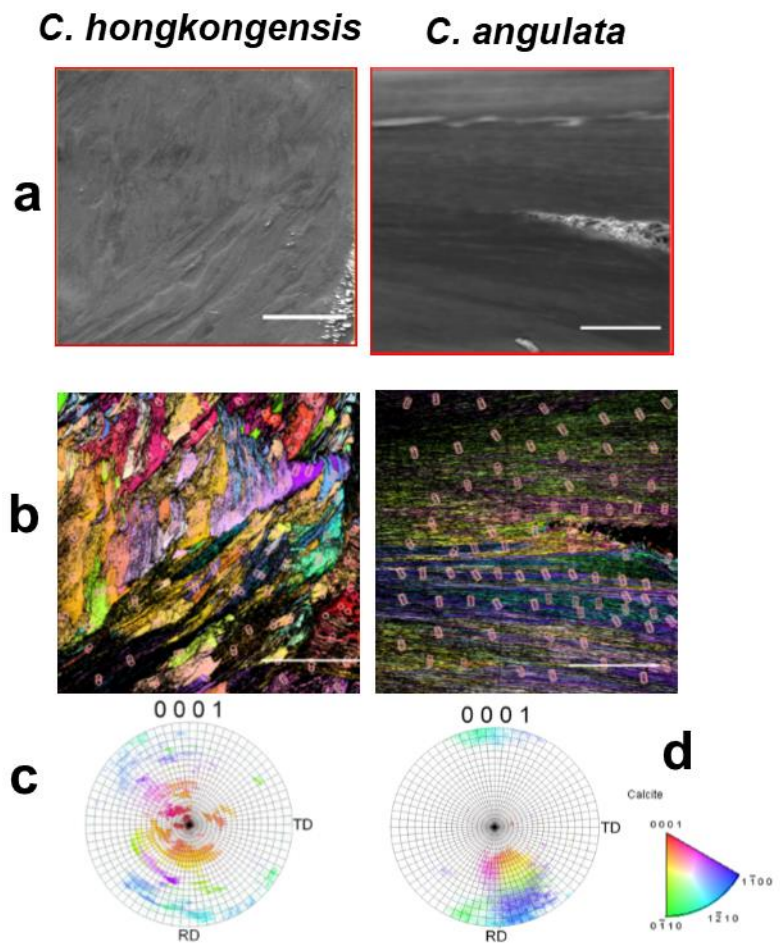

Figure 5. Comparison of shell crystallography of folia at the hinge of *C. hongkongensis* and *C. angulata* shells. Folia sections were imaged using SEM for (a) secondary electron images. SEM was also used for electron backscatter diffraction (EBSD) analyses of oyster shells for (b) crystallographic orientation maps with wire frames indicating crystal orientation corresponding to the colors of the map and (c) pole figures which correspond to the crystallographic orientation maps using the same color key showed in (d). Color key indicates the coding of the crystallographic planes for calcite; green {0 1 1 0}, blue {1 2 1 0}, red {1 1 0} planes.[40]

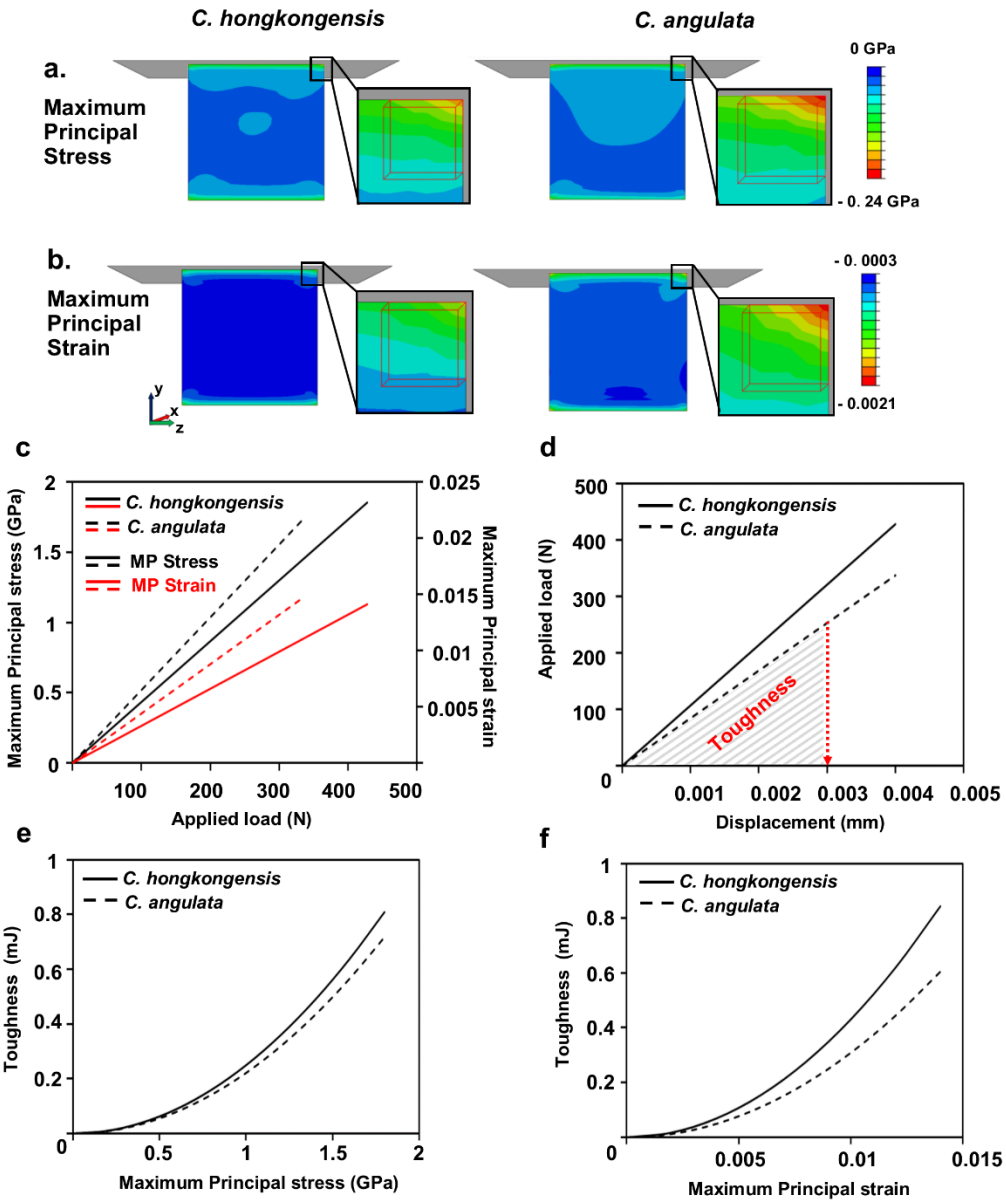

Figure 6. Finite element analysis of the mechanical behaviors of the folia cubes of *C. hongkongensis* and *C. angulata* shells under simulated compressive loading condition. The amplified vertex regions from the folia cube that exhibited (a) the calculated maximum principal (MP) stress distribution and (b) the calculated MP strain distribution of the of folia cube in *C. hongkongensis* and *C. angulata* shells under the same compressive force of 46. 8N with a rigid plane respectively. (c) the evolutionary MP stress peaks (black line) and MP strain peaks (red line) of folia cubes under compressive load in *C. hongkongensis* (solid line) and *C. angulata* (dashed line) shells. (d) the displacement (mm) - applied load (N) curve in which toughness is depicted. The toughness (required energy) of folia cubes in *C.*

hongkongensis (solid line) and *C. angulata* (dashed line) shells according to the MP stress peaks (e) and MP strain peaks (f) as failure criteria.

For Table of Contents Use Only

Crystallographic interdigitation in oyster shell folia enhances material strength

Yuan Meng,[†] Susan C. Fitzer,[#] Peter Chung,[§] Chaoyi Li,[†] Vengatesen Thiyagarajan,[†,]*and Maggie Cusack[‡,]*

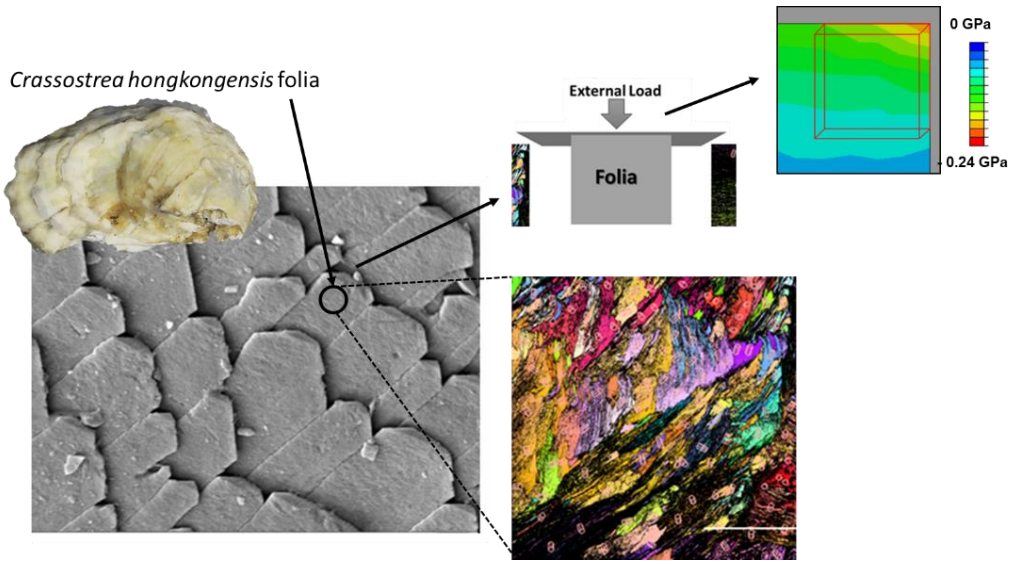

Folia are responsible for the mechanical support of edible oyster shells. Crystallographic interdigitations confer elevated mechanical strength in *C. hongkongensis* oyster shells compared to *C. angulata* shells by making *C. hongkongensis* concentrate less stress than the folia of *C. angulata* under same external load.